Change in Morphology of

Dimyristoylphosphatidylcholine / Bile Salt

Derivative Bicelle Assemblies with

Dodecylmaltoside in the Disk and Ribbon Phase

Wellington Leite<sup>1</sup>, Yuqi Wu<sup>2</sup>, Sai Venkatesh Pingali<sup>1</sup>, Raquel L. Lieberman<sup>2</sup>, Volker S. Urban<sup>1\*</sup>

<sup>1</sup> Neutron Scattering Division, Oak Ridge National Laboratory, 1 Bethel Valley Road, Oak Ridge, TN 37831, United States of America

<sup>2</sup> School of Chemistry & Biochemistry, Georgia Institute of Technology, 901 Atlantic Drive, Atlanta, GA 30332-0400, United States of America

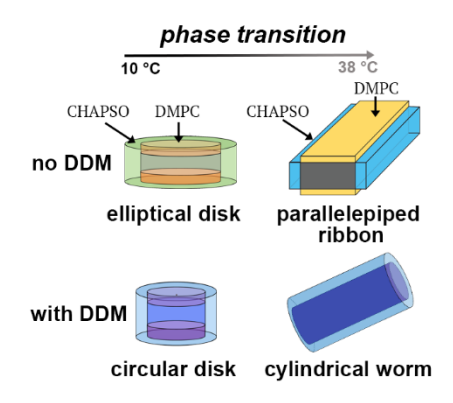
\*Corresponding author: urbanvs@ornl.gov or Raquel.lieberman@chemistry.gatech.edu

"This manuscript has been co-authored by UT-Battelle, LLC, under contract DE-AC05-00OR22725 with the US Department of Energy (DOE). The US government retains and the publisher, by accepting the article for publication, acknowledges that the US government retains a nonexclusive, paid-up, irrevocable, worldwide license to publish or reproduce the published form of this manuscript, or allow others to do so, for US government purposes. DOE will

provide public access to these results of federally sponsored research in accordance with the DOE Public Access Plan (<a href="http://energy.gov/downloads/doe-public-access-plan">http://energy.gov/downloads/doe-public-access-plan</a>).""

ABSTRACT: Bicelles, composed of a mixture of long and short chain lipids, form nanostructured molecular assemblies that are attractive lipid-membrane mimics for in *in vitro* studies of integral membrane proteins. Here we study the effect of a third component, single chain detergent n-dodecyl-b-D-maltoside (DDM) on the morphology of bicelles composed of 1,2-dimyristoyl-sn-glycero-3-phosphocholine (DMPC) and 3-((3-cholamidopropyl)dimethylammonio)-2-hydroxy-1-propanesulfonate (CHAPSO) below (10 °C) and above (38 °C) the phase transition. In the absence of DDM, bicelles convert from ellipsoidal disks at 10 °C to extended ribbon-like structures at 38 °C. The addition of DDM reshapes the ellipsoidal disc to a circular one and the flattened ribbon to a circular-cylinder worm-like micelle. Knowledge of the influence of the single chain detergent DDM on bicelle nanoscale morphology contributes towards comprehending lipid membrane self-organization and to the goal of optimizing lipid mimics for membrane biology research.

## **TOC GRAPHICS**



**KEYWORDS**: lipid, membrane, SANS, SAXS, self-assembly

The archetypical bicelle<sup>1</sup> is a nanostructured molecular assembly composed of a lipid bilayer disk, which in aqueous solution is edge-stabilized by a rim of detergent molecules<sup>1,2</sup>. Such systems mimic natural biological lipid bilayers and therefore are an important biophysical tool for preparations of integral membrane proteins in near-native state. The lipid molecule of choice has been 1,2-ditetradecanoyl-*sn*-glycero-3-phosphocholine (DMPC). Initially, the detergent was bile salt<sup>3</sup> or its zwitterionic derivative 3-([3-cholamidopropyl]dimethylammonio)-2-hydroxy-1-propanesulfonate (CHAPSO)<sup>4</sup> but later studies have predominantly used 1,2-dihexanoyl-*sn*-glycero-3-phosphocholine (DHPC)<sup>5</sup>. Recent studies suggest a revival of interest in CHAPSO as the detergent, thanks to improved stability of the resulting system<sup>1,6-9</sup>. One example is our previous study of an intramembrane aspartyl protease, which reveals a higher affinity of the enzyme to substrate in DMPC/CHAPSO as compared to a preparation with only n-dodecyl-β-D-maltoside (DDM) micelles.<sup>10</sup>

In addition to the bicelle disk, DMPC-detergent systems adopt many distinct nanoscopic morphologies. Such structures include ribbon, unilamellar vesicle, and multilamellar vesicle, and the resulting morphology depends on lipid to detergent ratio, lipid concentration, temperature, and solvent<sup>6, 11</sup>. Studies of such systems are interesting from a fundamental physical chemistry viewpoint due to the many interacting molecular forces that can be modified through the geometry and polarity of constituent molecular moieties, as well as temperature, solution conditions and addition of third component lipids or detergents.

This study contributes new molecular details regarding the arrangement of component molecules in DMPC/CHAPSO assemblies at 10 and 38 °C and addresses the effect of DDM on the detailed geometrical arrangement in the respective bicelle morphologies. Previous NMR studies examined the alignment of isotope labeled alkyl glycosides in bicelles<sup>5</sup>, which confirms that these molecules

insert in the bicelle above the gel-liquid transition temperature. However, the influence of these sugar-detergents on bicelle morphology has not been studied to the level of detail as presented in this Letter. Such knowledge is important in practice because membrane proteins are usually extracted initially from biological cell material with help of a mild detergent such as DDM, and then transferred into lipid bicelles for further study or use.

We studied the structural arrangement of 5% DMPC/CHAPSO bicelles (see Experimental Section) in the low-temperature phase (10 °C) with small-angle neutron scattering (SANS) in a contrast variation series. Deuterium-labeling, i.e., selectively replacing hydrogen atoms (H) with the heavier isotope deuterium (D) is a method in analytical techniques sensitive to isotopes, such as NMR spectroscopy, mass spectrometry, and neutron scattering. The isotope effect on molecular interactions is mild and often negligible, allowing broad applications of this method without noticeable effects on structure. A SANS signal is observed when structural features differ from the surrounding medium in their neutron scattering length density (SLD). The SLDs of H<sub>2</sub>O and D<sub>2</sub>O are -0.56 Å<sup>-2</sup> and 6.36 Å<sup>-2</sup>, respectively (Supporting Information (SI) Table S1). This large difference of SLDs allows varying neutron contrast between solutes and H<sub>2</sub>O/D<sub>2</sub>O over a wide range. In this study we used a series of H<sub>2</sub>O/D<sub>2</sub>O solutions with regular non-deuterated solutes and performed a repeat study with tail-deuterated d54-DMPC. The different contrast situations highlight different details of the molecular assemblies, yet importantly, all contrast situations agree with the same overall structural models. The contrast variation approach is illustrated by the simplified schematic representations in the insets of Figure 1C: At 18% D<sub>2</sub>O non-deuterated PC headgroups of d54-DMPC and CHAPSO are nearly contrast matched and scattering is strong from the deuterated d54-DM tails in the core of the bicelle; at 100% D<sub>2</sub>O contrast d54-DM is contrast matched and contrast is strongest for PC headgroups (top and bottom face of the bicelle); and at  $86\%~D_2O~d54\text{-DMPC}$  is on average contrast matched and contrast for the CHAPSO rim is strongest. The theoretical SLDs relevant to this study are found in SI Table S1.

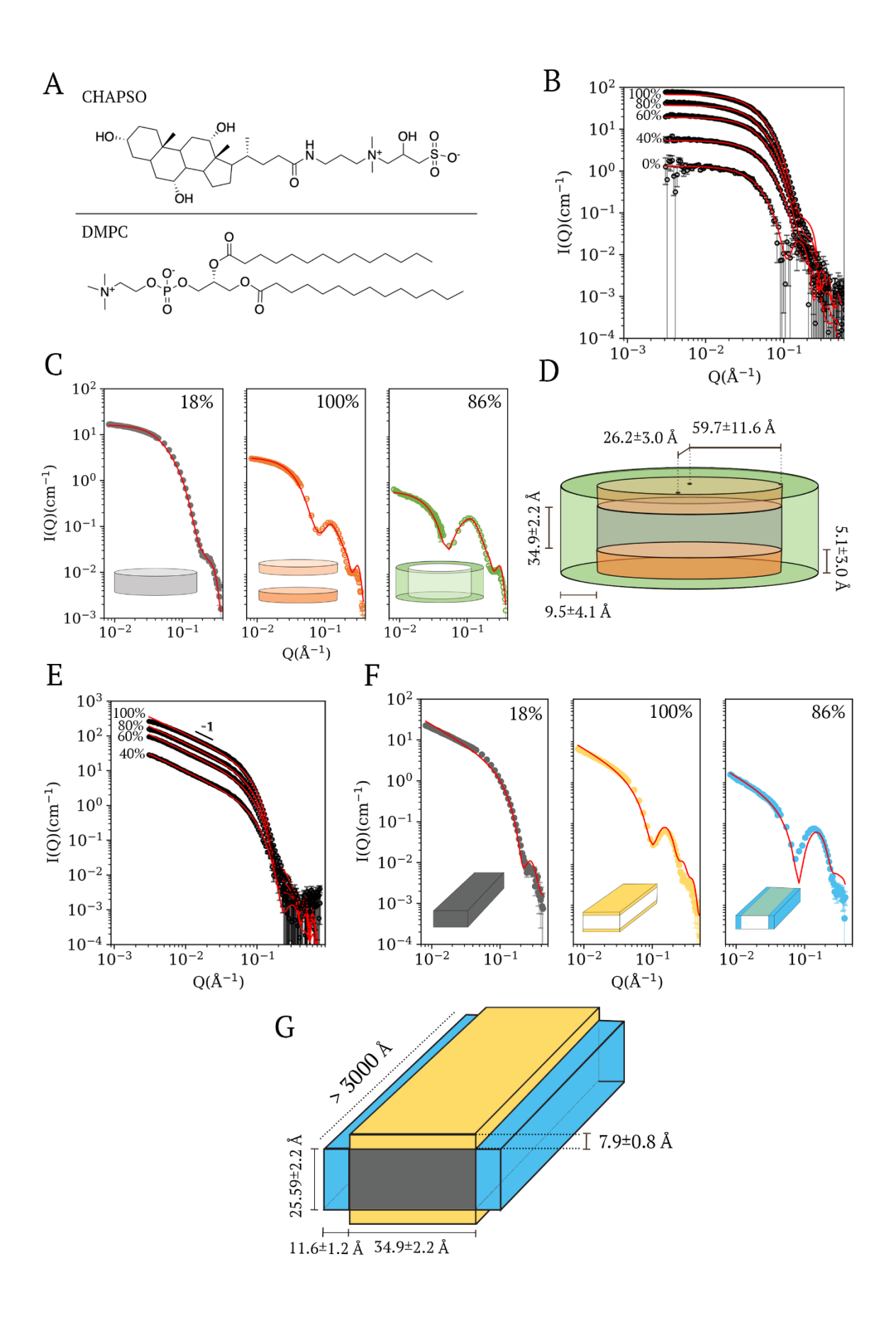


**Figure 1.** Arrangement of DMPC/CHAPSO in the low (10 °C) and high (38 °C) temperature phase. A) Chemical structure of lipid and detergent DMPC and CHAPSO, respectively. B) SANS profile of DMPC/CHAPSO at 10 °C in 100%, 80%, 60%, 40%, and 0% D<sub>2</sub>O buffers, shown with black circles. C) SANS profile of d54-DMPC/CHAPSO at 10 °C in 18% D<sub>2</sub>O shown with light gray circles, 100% D<sub>2</sub>O shown with orange circles, and 86% D<sub>2</sub>O shown with green circles. **D)** Elliptical cylinder core-shell model of DMPC/CHAPSO bicelle (not-to-scale). Hydrophobic core shown in light gray. Hydrophilic region containing lipid head group and detergent shown in orange and green, respectively. **E)** SANS profile of DMPC/CHAPSO at 38 °C in 100%, 80%, 60%, and 40% D<sub>2</sub>O buffers, shown with black circles. **F)** SANS profile of d54-DMPC/CHAPSO at 38 °C in 18% D<sub>2</sub>O shown with dark gray circles, 100% D<sub>2</sub>O shown with yellow circles, and 86% D<sub>2</sub>O shown with blue circles. **G)** Paralepidid core-shell model of DMPC/CHAPSO ribbons. Hydrophobic core shown in dark gray. Hydrophilic region containing lipid head group and detergent shown in yellow and blue, respectively. The theoretical SANS curves calculated for DMPC/CHAPSO bicelles and ribbons are shown as red lines.

SANS data, given as absolute scattering cross section as function of scattering vector magnitude (I vs Q, see Experimental Section) for the entire  $H_2O/D_2O$  contrast series is best fit simultaneously with an elliptical core-shell disk model indicating that 5% DMPC/CHAPSO adopts an elliptical disk-like arrangement (Figures 1B and D, Table 1). A circular disk model produces a significantly poorer fit result (SI Figure S1). We also performed Guinier analysis to yield a radius of gyration ( $R_g$ ). The results agree with the model fit (SI Figure S2, Table S2). The elliptical core has minor

and major semiaxes of  $26.2 \pm 3.0$  Å and  $59.7 \pm 11.6$  Å, respectively, and a height of  $34.9 \pm 2.2$  Å. The lipid bilayer aliphatic core is surrounded by a  $9.5 \pm 4.1$  Å and  $5.1 \pm 3.0$  Å thick shell formed by the detergent and lipid head group, respectively (Figure 1D, Table 1).

**Table 1**. Results from the simultaneous fit for the low–temperature phase samples

		Hydrophobi	c Core	Hydrophi		
	Model	Radius (Å)	Length (Å)	Lipid head group (Å)	Detergent (Å)	$\chi^2$
DMPC/CHAPSO	Elliptical Cylinder	26.2±3.0 and	34.9±2.2	5.1±3.0	9.5±4.1	90.9
		59.7±11.6*	34.9±2.2			
DMPC/CHAPSO/DDM	Circular Cylinder	33.3±1.9	34.9±2.7	5.1±3.2	9.0±3.5	78.77

 $<sup>\</sup>chi^2$  was calculated using simultaneous fit using the contrast variation series of protiated and deuterated samples and is normalized by the degree of freedoms. \* Long elliptical radius.

To gain additional structural resolution and confidence in the fitted models, next we conducted a SANS contrast variation series on a 5% DMPC/CHAPSO sample in which DMPC was replaced with tail-deuterated DMPC (d<sub>54</sub>-DMPC). Results from simultaneous fitting of SANS data for the d<sub>54</sub>-DMPC (Figure 1C and 1D, Table 1) agree with the non-deuterated system, confirming the prior elliptical cylinder core-shell model. In addition, analysis of the data from the d<sub>54</sub>-DMPC containing samples at the various D<sub>2</sub>O concentrations highlights different molecular features. At 100% D<sub>2</sub>O, the hydrophobic d<sub>54</sub>-DMPC tails that form the bilayer core are matched by the solvent SLD and scattering of the DMPC headgroups and CHAPSO is observed. A pronounced, so-called secondary maximum is observed in the SANS form factor. Such oscillations are commonly observed in SANS data from well-defined, simple geometric shapes. Importantly, a strong secondary peak

compared to the 'forward' intensity ( $Q \rightarrow 0$ ) furthermore is a hallmark of 'hollow' shapes with separated regions of correlated SLD. The position of this maximum represents a 'preferred' correlation distance ( $D \approx 2\pi/Q$ ), i.e.  $Q_{max} \approx 0.118 \text{ Å}^{-1}$  corresponds to an estimated spacing of  $D \approx 52.5 \text{ Å}$  (Figure 1C). This dominant correlation distance signifies frequent spacing between strongly scattering volume elements. Here the spacing reflects the distance between headgroups on two sides of the bilayer. At 86% D<sub>2</sub>O, the overall match point of d<sub>54</sub>-DMPC, highlights the arrangement of CHAPSO. These data reveal  $Q_{max} \approx 0.09 \text{ Å}^{-1}$  representing a CHAPSO-to-CHAPSO distance of 63 Å, ~10 Å longer than for DMPC head groups (Figure 1C). Thus, in accordance with the overall model CHAPSO is localized to the rim, separated from the DMPC bilayer in the bicelle. Finally, in 18% D<sub>2</sub>O, near the contrast match point of both CHAPSO (~20% D<sub>2</sub>O) and DMPC headgroups (34% D<sub>2</sub>O), (SI Table 1), SANS highlights the hydrophobic core structure from the deuterated tails of d<sub>54</sub>-DMPC, which shows an elongated shape with maximum dimension  $D_{max}$  of approximately 100 Å (SI Figure S3).

Analogous SANS data were measured above the phase transition of the 5% DMPC/CHAPSO and  $d_{54}$ -DMPC/CHAPSO, 38 °C. Unlike for the low temperature phase, there is a continuous and significant increase of intensity with decreasing scattering vector in the Q-range 0.003 to 0.07 Å<sup>-1</sup>, while at high Q the scattering signature remains similar (Figure 1E). Such an increase in intensity is consistent with formation of extended particles, in line with the ribbon bilayers previously proposed<sup>6</sup>. We note that for uniaxially extended scattering objects, such as rods or ribbons, a power law scattering exponent of  $Q^{-1}$  should be observed. However, the scattering intensity at low Q remains slightly below this limit, both in our work and that of others<sup>6</sup>. One potential explanation is an observation of finite length of these structures, but this would disagree with a long and intersected or packed ribbon model. Alternatively, a suppression of scattering intensity at low Q

may be observed due to repulsive steric or osmotic repulsion between ribbons. This appears plausible given the relatively concentrated systems and the competition of polar groups for solvation water. Further studies that employ osmotic screening could elucidate this aspect. We were able to model a ribbon form-factor for the SANS as a long core-shell parallelepiped. The parallelepiped hydrophobic core adopts a width and thickness of  $34.2\pm2.4$  Å and  $25.6\pm1.4$  Å, respectively (Figure 1E and 1G, Table 2). The long lipid bilayer aliphatic core is surrounded by a  $11.6\pm1.2$  Å and  $7.9\pm0.8$  Å thick shell formed by the detergent and lipid head group, respectively (Figure 1E and 1G, Table 2). The thickness of the lipid bilayer core ( $25.6\pm1.4$  Å) in the ribbon is less than the corresponding height dimension of the disk core ( $34.9\pm2.2$  Å). Previously X-ray scattering data on fluid phase bilayers composed of DMPC showed thermal contraction 12. The hydrophobic region of the DMPC bilayers ( $\sim25$  Å) at temperatures higher than 30 °C agrees well with our hydrophobic core thickness ( $25.6\pm1.4$  Å) in the ribbon phase. Thinning of the DMPC bilayer in the higher temperature phase above 22 °C is indeed expected to coincide with change in DMPC molecule dynamics at this phase transition 13.

**Table 2**. Results from the simultaneous fit for high–temperature phase samples.

		Core			Shell	Shell		
	Model	Thickness (Å)	Width (Å)	Long length (Å)	Lipid head g	Lipid head group (Å)		χ²
DMPC /CHAPSO	Parallel– epiped	25.6±1.4	34.2±2. 4	>3000	7.9±0.8		11.6±1.2	221
			Core			Shell		
		Model	Radius	(Å) l	Length (Å)	-	head group rgent (Å)	$\chi^2$
DMPC/CHA	APSO/DDM	Circular Cylinder	18.4±0.9	) :	>441±29	8.4±1.3	3	83.02

Initially, we tried an alternative model description as long cylinder with elliptical core-shell cross section as reported previously. This model gives less satisfactory fits over the complete data set (including deuterium-labeled and unlabeled assemblies), because it cannot account for the distinct localization of DMPC headgroups and CHAPSO on the wider and narrower surfaces of the ribbon, respectively. We can 'rescue' the elliptical model by introducing additional narrow strips for CHAPSO at the pointed ends of the elliptical cross section (see SI - Data Analysis and Modeling). However, the parallelepiped is simpler than this latter construct and should therefore be preferred for modeling the data. The low-Q data of DMPC/CHAPSO ribbons does not level off sufficiently in the measured SANS range to extract a reliable  $R_g$  value for the overall size of the assembly. The SANS window of observation ends at a  $Q_{min}$  of 0.003 Å-1 corresponding to a Bragg distance of 2000 Å. Thus, observed ribbon structures extend in length at least to this limit. The parallelepiped

model produced a good fit with a length of 3000 Å, but this value should be treated only as a lower limit estimate. Further analysis of the length dimension is hampered by a potential structure factor from repulsive interactions (see above).

The internal contrast in 5% d<sub>54</sub>-DMPC/CHAPSO at 38 °C emphasizes structural details of the assembly and agrees with the overall ribbon model. From data collected at 100% D<sub>2</sub>O it is apparent that CHAPSO and DMPC headgroups are separated by an average distance of 39.2 Å, which is 13.2 Å less than for the elliptical disk observed at 10 °C (Figure 1F, G and Figure 1C, D for high and low temperature phases, respectively). SANS profiles from samples in 86% D<sub>2</sub>O reveal a secondary maximum at  $Q_{max} \approx 0.13$  Å<sup>-1</sup>, corresponding to a CHAPSO separation of 48.3 Å, that is 9.1 Å larger than for the DMPC headgroups (39.2 Å). Thus, CHAPSO appears separated from DMPC also in the ribbon phase (Figure 1F and 1G).

Finally, we investigated the effect of adding DDM to 5% DMPC/CHAPSO at both 10 °C and 38 °C. DDM is a detergent commonly used in the study of functional membrane proteins <sup>14</sup> and is expected to be miscible with the long-chain DMPC. The final DDM concentration was 0.6% in the mixture and due to dilution, the DMPC/CHAPSO concentration was 4.7% in the following experiments. Rather than an elliptical disk, DDM-containing DMPC/CHAPSO bicelles at 10 °C exhibit SANS data consistent with a core of hydrophobic tails arranged as a circular disk shape. The hydrophobic core is a well-defined cylinder with a height and radius of 33.3±1.9 Å and 34.9±2.7 Å, respectively (Figures 2A and 2F). The dimensions of the hydrophilic shell formed by lipid head groups and detergents CHAPSO+DDM are  $5.1\pm3.2$  Å and  $9.0\pm3.5$  Å, respectively. These values are similar to that of bicelle without DDM (see Table 1). DMPC/CHAPSO samples in the presence of DDM were monodispersed as indicated by Guinier Analysis (Figure S4). Guinier analysis and P(r) curves yield  $R_g$  values of  $32.1\pm0.1$  Å and  $33.1\pm0.1$  Å, respectively, for DDM-

containing bicelle disks in 100% D<sub>2</sub>O (SI Figures S4, S5; SI Tables S2, S3). At 38 °C, the SANS results show that with added DDM the system still exhibits extended aggregates above the phase transition temperature (presence of DDM reduced the phase transition temperature by 2 °C, see SI Figure S6). SANS data were best fit with a circular cylinder core-shell SLD profile (Figure 2C, Table 2) with a hydrophobic core with radius of 18.4±0.9 Å and shell thickness of 8.4±1.3 Å. We can fit the cylinder length as 441 Å. However, this value must be interpreted with caution, and we report it here as a lower limit estimate of the possible length of the assembly (see above analogous discussion without DDM). SANS data from samples with d54-DMPC highlight the core-shell nature of the assembly (Figure 2B and 2D). The secondary peak positions indicate average headgroup spacing slightly smaller than without DDM. In sum, the effect of DDM on DMPC/CHAPSO is to convert the elliptical DMPC/CHAPSO disk into a circular one at low temperature and reduce the overall dimensions relative to the DMPC/CHAPSO ribbon at higher temperature.

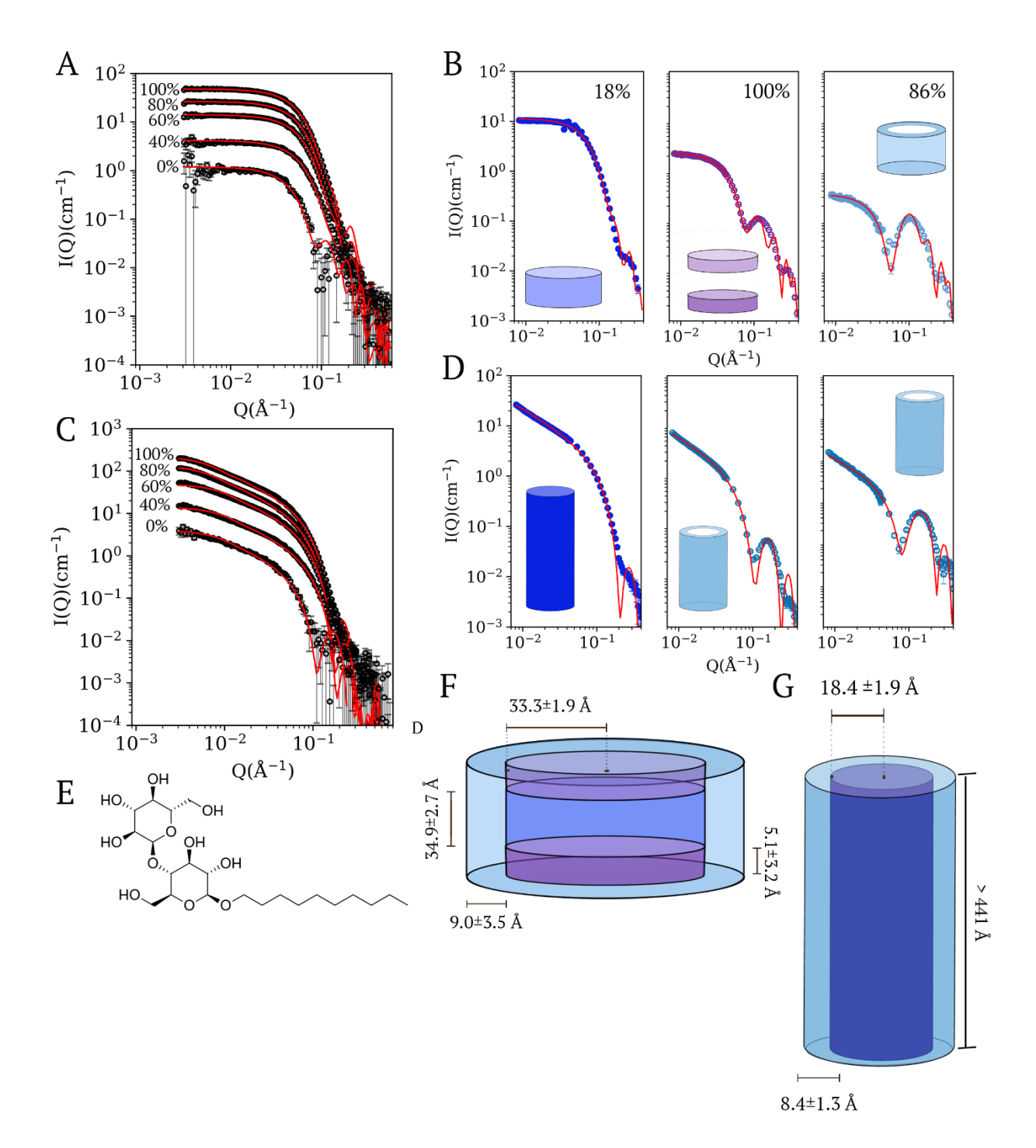


Figure 2. Arrangement of DMPC/CHAPSO/DDM in the low (10 °C) and high (38 °C) temperature phase. A) SANS profile of DMPC/CHAPSO at 10 °C in 100%, 80%, 60%, 40%, and 0% D<sub>2</sub>O buffers, shown with black circles. B) SANS profile of d54-DMPC/CHAPSO/DDM at 10 °C in 18% D<sub>2</sub>O shown with blue circles, 100% D<sub>2</sub>O shown with purple circles, and 86% D<sub>2</sub>O

shown with light blue circles. **C)** SANS profile of DMPC/CHAPSO/DDM at 38 °C in 100%, 80%, 60%, and 40% D<sub>2</sub>O buffers, shown with black circles. **D)** SANS profile of d54-DMPC/CHAPSO at 38 °C in 18% D<sub>2</sub>O shown with dark gray circles, 100% and 86% D<sub>2</sub>O shown with the same light blue circles as they represent the shell at different contrast condition. **E)** Chemical structure of detergent DDM. **F)** Circular cylinder core-shell model of DMPC/CHAPSO/DDM bicelle. The hydrophobic core is shown with blue color. The hydrophilic region containing lipid head group and detergent are shown with purple and light blue colors, respectively. **G)** Long circular cylinder core-shell model of DMPC/CHAPSO/DDM. Hydrophobic core shown in dark blue. Hydrophilic region containing mixed lipid head group and detergents shown in light blue. The theoretical SANS curves calculated for DMPC/CHAPSO bicelles and ribbons are shown as red lines.

Our study provides important new molecular details regarding DMPC/CHAPSO bicelles below and above the transition temperature from disks to ribbons<sup>6</sup>. We confirmed the location of CHAPSO at the rim of an elliptical bicelle disk at 10 °C and along the edges of a long ribbon at 38 °C. A driving force is required to promote and stabilize the elliptical shaped bicelles as compared to a circular cross section arrangement and this force should diminish as disorder increases<sup>15</sup>. The preference for elliptical bicelles at low temperature provides a rationale for unidirectional growth into ribbons across the phase transition. Beyond the scope of this study, it is not yet known whether a directional preference is imparted by the packing within the DMPC bilayer itself, or by the arrangement of CHAPSO at the rim. Previously, the ribbon phase was described as chiral nematic ribbon<sup>6</sup>. One driving force could be a tendency of CHAPSO to introduce a chiral twist in the ribbon as its molecules align to cover the rim. If this is the case, then fluid phase DMPC may more easily accommodate such a twist, while a solid-like lipid bilayer may

be too rigid. This could limit the achievable length of the low temperature assembly to elliptical disks. Earlier studies explained the disk to ribbon phase transition as due to reduced availability of edge-stabilizing CHAPSO, which becomes more soluble in the DMPC at higher temperature<sup>6</sup>. However, this cannot explain why larger aggregates grow as 1-dimensional ribbons rather than simply expand to larger bicelle disks.

Our study is the first to investigate molecular perturbations to DMPC/CHAPSO bicelles upon introduction of DDM, a common reagent used during the purification of membrane proteins. A 3-component system would be expected to have higher entropy than DMPC/CHAPSO alone, and this should drive the system towards a more isotropic arrangement. Indeed, the addition of DDM results in a disk with a circular cross section of narrower diameter at low temperature than DMPC/CHAPSO lacking DDM. Importantly, the admixture with DDM still adopts an overall disk shape at 10 °C or a ribbon at 38 °C, and clearly distinct from highly curved<sup>6</sup>, oblate DDM micelles<sup>16</sup>. This finding is consistent with the notion that it is the bilayer-like plane in bicelles that stabilizes membrane proteins in functional state<sup>2, 17-19</sup>.

The results with DDM raises the possibility that there may be a limit to the size of a membrane protein that can be successfully hosted in a DMPC/CHAPSO bicelle. Lipid assemblies are highly sensitive to perturbation, as demonstrated here with the addition of DDM, with the addition of organic biomolecules<sup>20</sup>, peptides<sup>21</sup>, or even during processes such as membrane protein crystallization<sup>15</sup>. Thus, the presence of the membrane protein itself may alter the structure of bicelle lipid assemblies to provide a custom fit, a direction for future investigations. In the long term, a better fundamental understanding of the physical factors that affect the shape, size, and fluidity of lipids and their synthetic mimics will contribute to the development of rationally-selected and optimized lipid mixtures for biomembrane research.

# **EXPERIMENTAL METHODS**

We prepared 5% (w/v) DMPC/CHAPSO (2.8:1 molar ratio, 3 mass ratio) in 20 mM HEPES pH 7.5, 250 mM NaCl according to literature procedures<sup>22</sup>. DDM containing samples were prepared by mimicking the procedure used in biochemical assays<sup>10, 23</sup>. Briefly, on ice, a stock solution of DDM was diluted ~17x to a final concentration of 4.7% DMPC/CHAPSO and 0.6% DDM.

Samples were prepared for two SANS contrast series. The first set of data used regular protiated lipids and surfactants prepared in D<sub>2</sub>O/H<sub>2</sub>O mixtures between 0 to 100 % D<sub>2</sub>O (see Suppl Tabl1 1). A second set of samples employed DMPC and DDM with perdeuterated tail groups (d<sub>54</sub>-DMPC, d<sub>25</sub>-DDM), likewise prepared in series of D<sub>2</sub>O/H<sub>2</sub>O mixtures.

SANS data were measured at the CG-3 Bio-SANS instrument of Oak Ridge National Laboratory<sup>24</sup>. SANS samples were 300 microliter aliquots contained cylindrical quartz cuvettes with 1mm pathlength. Neutron wavelength ( $\lambda$ ) was 6 Å +/- 14% (FWHM) and beam spot size on sample was defined by 14 mm diameter circular aperture. Sample to detector distance was 1m and 15m for the wing and main detector, respectively. The instrument settings provide a continuous range of momentum transfer values Q from 0.003 to 1 Å<sup>-1</sup> ( $Q = 4\pi \sin(\theta/2) / \lambda$ ,  $\theta$  is the scattering angle, i.e., the angle between beam axis and scattered neutron trajectory). Data reduction followed established protocols to yield absolute scattering cross sections as function of Q. SANS data analysis was performed by fitting cylinder or parallelepiped models in SASVIEW, http://www.sasview.org/. Additional model-independent data analysis included linearized Guinier fits and pair distribution (P(r)), where appropriate (see SI - Data Analysis and Modeling for details).

### ASSOCIATED CONTENT

# **Supporting Information**

The Supporting Information is available free of charge.

Details of sample preparation, SANS and DSC experiment techniques, data analysis, figures, tables, and references (PDF)

# **AUTHOR INFORMATION**

# **Corresponding Authors**

Volker S. Urban, Neutron Scattering Division, Oak Ridge National Laboratory, 1 Bethel Valley Road, Oak Ridge, TN 37831; orcid.org/0000-0002-7962-3408

Email: urbanvs@ornl.gov

Raquel L. Lieberman, School of Chemistry & Biochemistry, Georgia Institute of Technology, 901 Atlantic Drive, Atlanta, GA 30332-0400; orcid.org/0000-0001-9345-3735

Email: Raquel.lieberman@chemistry.gatech.edu

# **Authors**

Wellington C. Leite, Neutron Scattering Division, Oak Ridge National Laboratory, 1 Bethel Valley Road, Oak Ridge, TN 37831; ResearcherID: B-4996-2018

Yuqi Wu, School of Chemistry & Biochemistry, Georgia Institute of Technology, 901 Atlantic Drive, Atlanta, GA 30332-0400

Sai Venkatesh Pingali, Neutron Scattering Division, Oak Ridge National Laboratory, 1 Bethel Valley Road, Oak Ridge, TN 37831; orcid.org/0000-0001-7961-4176

### **Notes**

The authors declare no competing financial interests.

### ACKNOWLEDGMENT

This work was supported by NSF grant 1817796 to RLL. This work benefited from the use of the SasView application, originally developed under NSF award DMR-0520547. SasView contains code developed with funding from the European Union's Horizon 2020 research and innovation programme under the SINE2020 project, grant agreement No 654000. Neutron scattering studies at the CG-3 Bio-SANS instrument at the High-Flux Isotope Reactor operated by the Oak Ridge National Laboratory were sponsored by the Office of Biological and Environmental Research and by the Scientific User Facilities Division, Office of Basic Energy Sciences, U.S. Department of Energy. This manuscript has been co-authored by UT-Battelle, LLC under Contract No. DE-AC05-00OR22725 with the U.S. Department of Energy. The United States Government retains and the publisher, by accepting the article for publication, acknowledges that the United States Government retains a nonexclusive, paid-up, irrevocable, worldwide license to publish or reproduce the published form of this manuscript, or allow others to do so, for United States Government purposes. The Department of Energy will provide public access to these results of federally sponsored research in accordance with the DOE Public Access Plan (http://energy.gov/downloads/doepublic- access-plan). We thank Dr. Haden Scott for assistance with conducting DSC measurements.

## REFERENCES

- (1) Sanders, C. R., II; Landis, G. C. Reconstitution of membrane proteins into lipid-rich bilayered mixed micelles for NMR studies. *Biochemistry* **1995**, *34* (12), 4030-4040.
- (2) Sanders, C. R., II; Hare, B. J.; Howard, K. P.; Prestegard, J. H. Magnetically-oriented phospholipid micelles as a tool for the study of membrane-associated molecules. *Prog. Nucl. Magn. Reson. Spectrosc.* **1994**, *26*, 421-444.
- (3) Ram, P.; Prestegard, J. H. Magnetic field induced ordering of bile salt/phospholipid micelles: new media for NMR structural investigations. *Biochim. Biophys. Acta Biomembr.* **1988**, *940* (2), 289-294.
- (4) Sanders, C. R., 2nd; Prestegard, J. H. Magnetically orientable phospholipid bilayers containing small amounts of a bile salt analogue, CHAPSO. *Biophys. J.* **1990**, *58* (2), 447-460.
- (5) Sanders, C. R., 2nd; Schwonek, J. P. Characterization of magnetically orientable bilayers in mixtures of dihexanoylphosphatidylcholine and dimyristoylphosphatidylcholine by solid-state NMR. *Biochemistry* **1992**, *31* (37), 8898-8905.
- (6) Li, M.; Morales, H. H.; Katsaras, J.; Kučerka, N.; Yang, Y.; Macdonald, P. M.; Nieh, M. P. Morphological characterization of DMPC/CHAPSO bicellar mixtures: A combined SANS and NMR study. *Langmuir* **2013**, *29* (51), 15943-15957.
- (7) Czerski, L.; Sanders, C. R. Functionality of a membrane protein in bicelles. *Anal. Biochem.* **2000**, *284* (2), 327-333.
- (8) Cavagnero, S.; Dyson, H. J.; Wright, P. E. Improved low pH bicelle system for orienting macromolecules over a wide temperature range. *J. Biomol. NMR* **1999**, *13* (4), 387-391.
- (9) Wang, H.; Eberstadt, M.; Olejniczak, E. T.; Meadows, R. P.; Fesik, S. W. A liquid crystalline medium for measuring residual dipolar couplings over a wide range of temperatures. *J. Biomol. NMR* **1998**, *12* (3), 443-446.
- (10) Naing, S.-H.; Kalyoncu, S.; Smalley, D. M.; Kim, H.; Tao, X.; George, J. B.; Jonke, A. P.; Oliver, R. C.; Urban, V. S.; Torres, M. P.; et al. Both positional and chemical variables control in vitro proteolytic cleavage of a presentilin ortholog. *J. Biol. Chem.* **2018**, *293* (13), 4653-4663.
- (11) Katsaras, J.; Harroun, T. A.; Pencer, J.; Nieh, M. P. "Bicellar" lipid mixtures as used in biochemical and biophysical studies. *Naturwissenschaften* **2005**, *92* (8), 355-366.
- (12) Kučerka, N.; Nieh, M.-P.; Katsaras, J. Fluid phase lipid areas and bilayer thicknesses of commonly used phosphatidylcholines as a function of temperature. *Biochim. Biophys. Acta Biomembr.* **2011**, *1808* (11), 2761-2771.

- (13) Sharma, V. K.; Mamontov, E.; Anunciado, D. B.; O'Neill, H.; Urban, V. Nanoscopic dynamics of phospholipid in unilamellar vesicles: effect of gel to fluid phase transition. *J. Phys. Chem. B* **2015**, *119* (12), 4460-4470.
- (14) Prive, G. G. Detergents for the stabilization and crystallization of membrane proteins. *Methods* **2007**, *41* (4), 388-397.
- (15) Murugova, T. N.; Ivankov, O. I.; Ryzhykau, Y. L.; Soloviov, D. V.; Kovalev, K. V.; Skachkova, D. V.; Round, A.; Baeken, C.; Ishchenko, A. V.; Volkov, O. A.; et al. Mechanisms of membrane protein crystallization in 'bicelles'. *Sci. Rep.* **2022**, *12* (1), 11109.
- (16) Oliver, R. C.; Lipfert, J.; Fox, D. A.; Lo, R. H.; Doniach, S.; Columbus, L. Dependence of micelle size and shape on detergent alkyl chain length and head group. *PLoS One* **2013**, *8* (5), e62488.
- (17) Vold, R. R.; Prosser, R. S. Magnetically oriented phospholipid bilayered micelles for structural studies of polypeptides. Does the ideal bicelle exist? *J. Magn. Reson. B* **1996**, *113*, 267-271.
- (18) Luchette, P. A.; Vetman, T. N.; Prosser, R. S.; Hancock, R. E.; Nieh, M. P.; Glinka, C. J.; Krueger, S.; Katsaras, J. Morphology of fast-tumbling bicelles: a small angle neutron scattering and NMR study. *Biochim. Biophys. Acta* **2001**, *1513* (2), 83-94.
- (19) Piai, A.; Fu, Q.; Dev, J.; Chou, J. J. Optimal Bicelle Size q for Solution NMR Studies of the Protein Transmembrane Partition. *Chemistry* **2017**, *23* (6), 1361-1367.
- (20) Sharma, V. K.; Mamontov, E.; Tyagi, M.; Urban, V. S. Effect of alpha-Tocopherol on the Microscopic Dynamics of Dimyristoylphosphatidylcholine Membrane. *J. Phys. Chem. B* **2016**, *120* (1), 154-163.
- (21) Sharma, V. K.; Mamontov, E.; Tyagi, M.; Qian, S.; Rai, D. K.; Urban, V. S. Dynamical and Phase Behavior of a Phospholipid Membrane Altered by an Antimicrobial Peptide at Low Concentration. *J. Phys. Chem. Lett.* **2016**, *7* (13), 2394-2401.
- (22) Ujwal, R.; Bowie, J. U. Crystallizing membrane proteins using lipidic bicelles. *Methods* **2011**, *55* (4), 337-341.
- (23) Naing, S.-H.; Vukoti, K. M.; Drury, J. E.; Johnson, J. L.; Kalyoncu, S.; Hill, S. E.; Torres, M. P.; Lieberman, R. L. Catalytic Properties of Intramembrane Aspartyl Protease Substrate Hydrolysis Evaluated Using a FRET Peptide Cleavage Assay. *ACS Chem. Biol.* **2015**, *10* (9), 2166-2174.
- (24) Heller, W. T.; Urban, V. S.; Lynn, G. W.; Weiss, K. L.; O'Neill, H. M.; Pingali, S. V.; Qian, S.; Littrell, K. C.; Melnichenko, Y. B.; Buchanan, M. V.; et al. The Bio-SANS instrument at the High Flux Isotope Reactor of Oak Ridge National Laboratory. *J. Appl. Crystallogr.* **2014**, *47*, 1238-1246.